



## Effects of Cr content on microstructure and mechanical properties of single crystal superalloy

Zhen-xue SHI, Shi-zhong LIU, Xiao-guang WANG, Jia-rong LI

Science and Technology on Advanced High Temperature Structural Materials Laboratory,  
Beijing Institute of Aeronautical Materials, Beijing 100095, China

Received 24 April 2014; accepted 25 September 2014

**Abstract:** Two experimental single crystal superalloys with 2% Cr and 4% Cr (mass fraction) were cast in a directionally solidified furnace, while other alloying element contents were kept unchanged. The effects of Cr content on the microstructure, phase stability, tensile properties at 1100 °C and stress rupture properties at 1070 °C and 160 MPa of the single crystal superalloy were investigated. The results show that the size of  $\gamma'$  phase particles become small and uniform, and the cubic shape turns a little regular with the increase of Cr content. The  $\gamma'$  directional coarsening and rafting were observed in the 2% Cr and 4% Cr alloys after long term aging (LTA) at 1100 °C. The rafting rate of  $\gamma'$  phase increased with increasing Cr content. Needle-shaped topologically close packed (TCP) phases precipitated and grew along fixed direction in both alloys. The precipitating rate and volume fraction of TCP phases significantly increased with the increase of Cr content. The tensile property of the alloy increased and the stress rupture properties of the alloy decreased with the increase of Cr content at high temperature. The increase of Cr content increased the partition ratio of TCP forming elements, Re, W, and Mo, and the saturation degrees of these elements in  $\gamma$  phases increased. Therefore, the high temperature phase stability of the alloy decreased with the increase of Cr content.

**Key words:** single crystal superalloy; Cr content; microstructure; phase stability; mechanical properties

### 1 Introduction

In recent years, Ni-based single crystal superalloys have become a major material for the blades in aerospace turbine engines. The demand for enhanced high temperature mechanical strength in these alloys has led to increasingly higher additions of refractory alloying elements to enhance the degree of solid solution strengthening [1,2]. On the other hand, Cr levels have been reduced to compensate for elevated levels of refractory alloying elements in order to avoid the formation of topologically close packed (TCP) phases, which decrease the stress rupture properties of the alloy by serving as crack initiation sites [3,4]. For example, the mass fractions of Cr in the single crystal superalloys from the first generation to the third generation, i.e., CMSX-2, CMSX-4 to CMSX-10, are 8.0%, 6.5% and 2.3%, respectively [5]. The fourth generation single crystal superalloys, such as MC-NG, EPM-102, and TMS-138, contain 2% Cr, respectively [6–8]. However, lower Cr content results in the decrease of oxidation

resistance and poorer corrosion resistance; thus, it has become increasingly difficult to develop new single crystal superalloys with a balanced combination of strength, environmental resistance, castability and microstructural stability [9]. The research about the effect of Cr content on the microstructure and mechanical properties of single crystal superalloys has been rather limited [10–12]. So, it is meaningful to systematically investigate the action of Cr in the single crystal superalloys with high level refractory alloy elements. The present study examined the effect of Cr content on the microstructure, phase stability, tensile properties and stress rupture properties of a Ni-based single crystal superalloy, with the aim to promote the development of new generation single crystal superalloy with high microstructure stability and good mechanical properties.

### 2 Experimental

Pure raw materials were used in the experiment. Two Ni–Cr–Co–Mo–W–Ta–Nb–Re–Al systems with

single crystal and [001] orientation were cast by crystal selection method in the directionally solidified furnace with high temperature gradient of 80 °C/cm. The Cr contents of two alloys are 2% and 4% (mass fraction), respectively, and the chemical compositions of other alloy elements are the same. The nominal chemical compositions of experimental alloys are shown in Table 1. The crystal orientations of the specimens were determined with Laue X-ray back reflection method, and the crystal orientation deviations of the specimens were maintained within 10° from the [001] orientation. The single crystal specimens received the same standard heat treatment comprising of a solution treatment (1345 °C, 6 h, AC) and a two-step aging treatment (1120 °C, 4 h, AC) + (870 °C, 24 h, AC). Then, the alloys were long term aged at 1100 °C for 50, 100, 200, 400 and 800 h, respectively. The standard cylindrical specimens for tensile and stress rupture tests were machined after heat treatment. The tensile and stress rupture tests were conducted at 1100 °C and 1070 °C, 160 MPa in air using a DST-5 testing machine with furnace attachment, respectively. The samples were etched with 5 g CuSO<sub>4</sub> + 25 mL HCl + 20 mL H<sub>2</sub>O + 5 mL H<sub>2</sub>SO<sub>4</sub> which dissolves the  $\gamma'$  phase. Microstructures of the alloys under different conditions were examined by using an S4800 scanning electron microscope.

**Table 1** Nominal chemical compositions of experimental alloys

Alloy	Mass fraction/%				
	Cr	Co	Mo	W	Ta
2% Cr	2	7–10	2–5	6–9	7–10
4% Cr	4	7–10	2–5	6–9	7–10
Alloy	Re	Nb	Al	Hf	Ni
2% Cr	3–5	0.5–1.5	5–6	0.1–0.5	Bal.
4% Cr	3–5	0.5–1.5	5–6	0.1–0.5	Bal.

### 3 Results and discussion

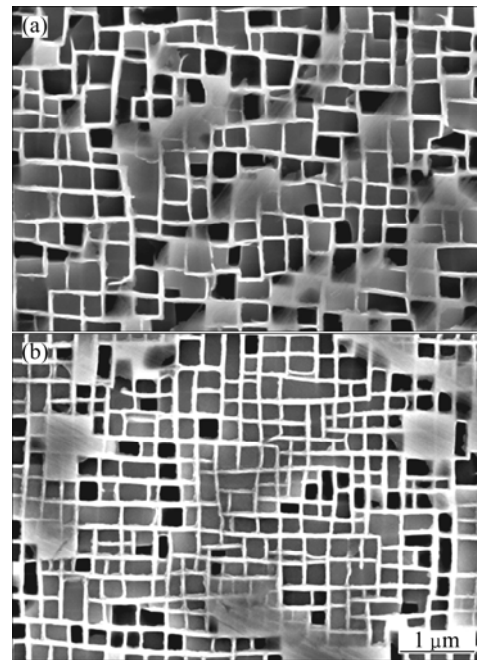
#### 3.1 Microstructure after full heat treatment

Figure 1 shows the typical microstructures of the 2% Cr alloy and 4% Cr alloy after full heat treatment. It can be seen that the primary  $\gamma'$  and  $\gamma/\gamma'$  eutectic dissolve completely after the high temperature solution treatment. They contain more than 60%  $\gamma'$  phase in cubic shape and  $\gamma$  matrix channel. The average  $\gamma'$  phase sizes of two alloys are 0.54 and 0.43  $\mu\text{m}$ , respectively. The size of  $\gamma'$  phase particles becomes small and uniform, and the cubic shape turns regular with increasing Cr content. Therefore, the  $\gamma$  matrix channel of the 4% Cr alloy is a little straighter than that of the 2% Cr alloy.

#### 3.2 Microstructure after long term aging

Figures 2 and 3 illustrate the microstructures of (001) plane of the 2% Cr alloy and 4% Cr alloys after

long term aging (LTA) at 1100 °C for 50, 100, 200, 400, and 800 h, respectively.



**Fig. 1** SEM images of alloys after full heat treatment: (a) 2% Cr; (b) 4% Cr

It can be seen from Fig. 2 that with prolonging time the size of  $\gamma'$  precipitate in the 2% Cr alloy gradually became larger and its morphology was still in cubic shape after long term aging of 200 h. The lateral merging of  $\gamma'$  precipitates had begun along the cubic direction. After 400 h, adjacent  $\gamma'$  particles met and fused together, producing extended rafts or plates. The  $\gamma$  phase became no longer continuous and was thus entirely surrounded by the  $\gamma'$  phase. It can be seen from Fig. 3 that rafts had already formed in the 4% Cr alloy after long term aging of 200 h. It can be seen through comparison of the two alloys that the coarsening extent of  $\gamma'$  phases became more severe with increasing Cr content.

The microstructure of Ni-based single crystal superalloy changed significantly after LTA at high temperature. The  $\gamma'$  directional coarsening and rafting can be observed in this process. The  $\gamma'$  coarsening and rafting are attributed to the directional diffusion of the alloying elements at elevated temperature. Coherency stresses due to the lattice misfit between  $\gamma$  and  $\gamma'$  phases act as the driving force for these microstructural changes [13]. Because of slight differences in lattice constants of both  $\gamma$  and  $\gamma'$  phases, a lattice misfit exists. It is well known that the lattice misfit of Ni-based superalloys is strongly influenced by the alloy composition. The alloying element Cr can increase the amount of lattice misfit as it partitions preferentially to the  $\gamma$  matrix [11]. Therefore, the rafting rate of  $\gamma'$  phase increases with increasing Cr content.

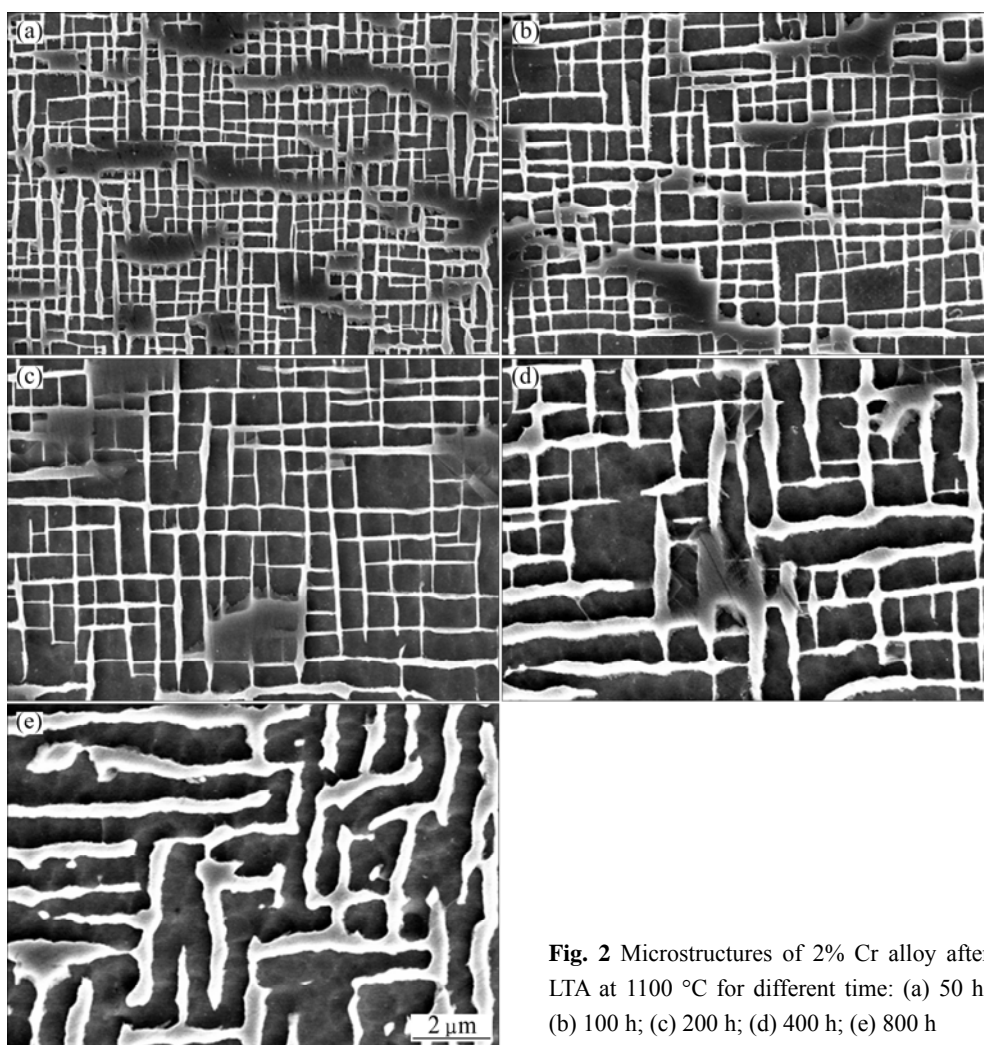


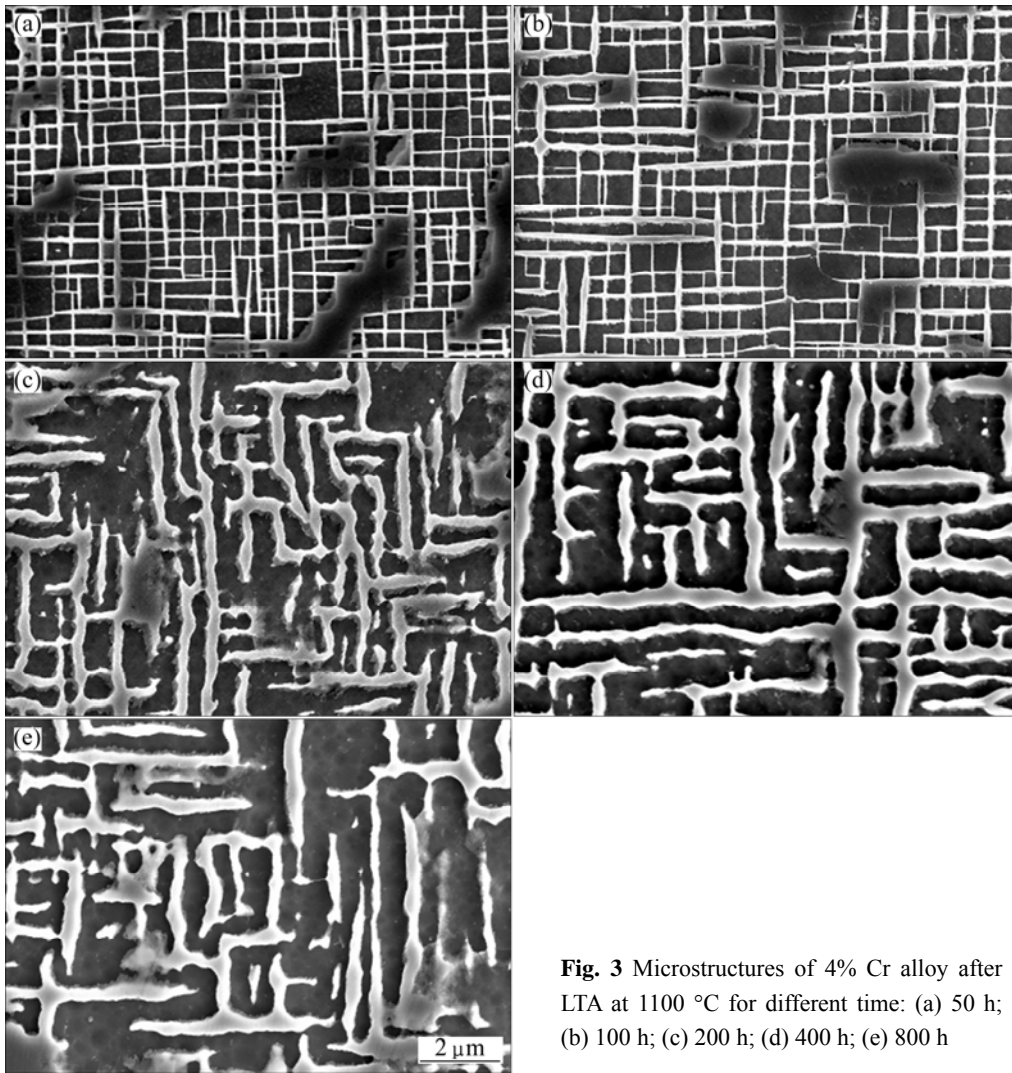
**Fig. 2** Microstructures of 2% Cr alloy after LTA at 1100 °C for different time: (a) 50 h; (b) 100 h; (c) 200 h; (d) 400 h; (e) 800 h

The microstructure stability at elevated temperatures is a key concern for the single crystal superalloys. Figure 4 illustrates the TCP precipitates in the alloys after LTA at 1100 °C. It can be seen that TCP phase precipitated much less in the 2% Cr alloy than in the 4% Cr alloy after LTA. Moreover, the precipitating rate of TCP phases was significantly influenced by Cr content. In the 2% Cr alloy, the onset of TCP precipitation occurred after aging at 1100 °C for 400 h. However, the onset of TCP precipitation occurred after aging at 1100 °C for 100 h in the 4% Cr alloy. This indicates that the increase of Cr content to Ni-based single crystal superalloy with high refractory content can decrease high temperature phase stability.

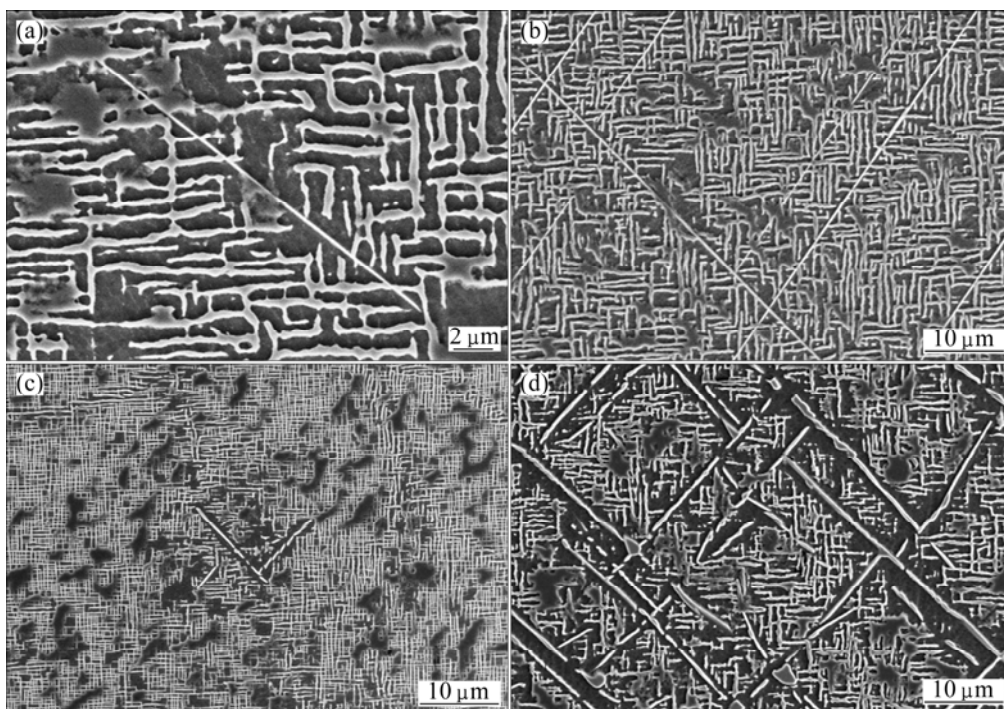
The chemical compositions of TCP phases in the 2% Cr and 4% Cr alloys after LTA at 1100 °C for 800 h using SEM equipped with an energy-dispersive X-ray spectroscopy (EDS) are shown in Table 2. Every datum is the mean value of five tests. It is shown that in both of the alloys, Re, W, Co, and Mo are enriched in the TCP phases.

The formation of TCP phases in Ni-based single

crystal superalloys has generally been attributed to the supersaturation of high melting point refractory elements (Re, W, Mo) within the disordered  $\gamma$  phase [14]. As the levels of these refractory alloying additions are increased to enhance the creep properties of single crystal superalloys, the limited degree of refractory element solubility within the  $\gamma'$  phase increased. After the standard heat treatment of the 2% Cr and 4% Cr alloys, the compositions of  $\gamma$  and  $\gamma'$  phases were measured using EDS analysis equipment attached to SEM. The comparison of the partition ratio of alloying element in the two alloys is shown in Fig. 5. The partition ratio is given by  $k_i = C_{i\gamma}/C_{i\gamma'}$ , where  $i$  corresponds to a particular element,  $C_{i\gamma}$  and  $C_{i\gamma'}$  correspond to the concentration of alloying element  $i$  in the  $\gamma$  and  $\gamma'$  phases, respectively. It can be seen from Fig. 5 that the distribution behavior of the same element in  $\gamma$  and  $\gamma'$  phases is similar in the 2% Cr and 4% Cr alloys. The main solid solution strengthening elements W, Mo, and particularly Re are enriched in the  $\gamma$  matrix. Cr has also been found to partition preferentially into the  $\gamma$  matrix. The increase of Cr content raises the partition ratio of TCP forming



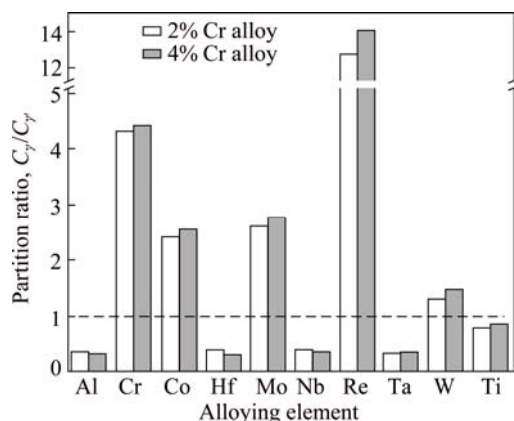
**Fig. 3** Microstructures of 4% Cr alloy after LTA at 1100 °C for different time: (a) 50 h; (b) 100 h; (c) 200 h; (d) 400 h; (e) 800 h



**Fig. 4** TCP precipitates in alloys after LTA at 1100 °C: (a) 2% Cr, 400 h; (b) 2% Cr, 800 h; (c) 4% Cr, 100 h; (d) 4% Cr, 800 h

**Table 2** Chemical compositions of TCP phase in 2% Cr and 4% Cr alloys

Alloy	Mass fraction/%						Ni
	Al	Cr	Co	Mo	Re	W	
2% Cr	4.4	1.7	8.1	3.5	22.4	13.1	Bal.
4% Cr	4.8	2.9	7.7	3.1	25.7	12.5	Bal.

**Fig. 5** Partition ratio of alloying element in 2% Cr and 4% Cr alloys

elements, Re, W, and Mo. Therefore, the saturation degrees of Re, W and Mo increase with increasing Cr content, which can enable 4% Cr alloy to be easy to the formation of TCP phases. This is in good agreement with measurements carried out by CHEN et al [11].

### 3.3 Tensile properties

The tensile properties of 2% Cr and 4% Cr alloys aged at 1100 °C are shown in Table 3. It can be seen that the yield strength and tensile strength increase, while elongation and contraction of area decrease with increasing Cr content.

**Table 3** Tensile properties of 2% Cr and 4% Cr alloys aged at 1100 °C

Alloy	$\sigma_{0.2}$ /MPa	$\sigma_b$ /MPa	$\delta$ /%	$\psi$ /%
2% Cr	491	569	44.0	48.4
4% Cr	528	590	20.7	44.3

$\psi$  is contraction of area

The difference of tensile properties of 2% Cr and 4% Cr alloys can largely be attributed to the change of microstructure by Cr content. The Ni-based single crystal superalloy is mainly strengthened by  $\gamma'$  phase. The tensile property of single crystal superalloy is strongly affected by the size and shape of  $\gamma'$  phase. The size of  $\gamma'$  phase particles becomes small and uniform and the cubic shape of  $\gamma'$  phase particles turns a little regular with increasing Cr content. Moreover, the lattice misfit has an important relation with mechanical property for the single crystal superalloy at high temperature. The magnitude of the

lattice misfit controls the density of the interfacial dislocations required to relieve the misfit stresses. The alloying element Cr increases the amount of lattice misfit because it partitions preferentially to the  $\gamma$  matrix, as shown in Fig. 5. The  $\gamma/\gamma'$  interface is the obstacle of dislocation movement [15]. With the decrease of the size of  $\gamma'$  particles, the strengthening effect increases. Therefore, the solid strengthening effect in the 4% Cr alloy is larger than that in 2% Cr alloy. The tensile property of 4% Cr alloy is better than that of 2% Cr alloy at high temperature.

### 3.4 Stress rupture properties

The stress rupture properties of 2% Cr and 4% Cr alloys aged at 1070 °C and 160 MPa are shown in Table 4. It can be seen that the stress rupture lives and elongations all decrease with increasing Cr content.

**Table 4** Stress rupture properties of 2% Cr and 4% Cr alloys aged at 1070 °C and 160 MPa

Alloy	$t$ /h	$\delta$ /%	$\psi$ /%
2% Cr	491.0	23.8	42.2
4% Cr	388.8	15.8	30.1

The microstructures on the longitudinal section in the ruptured specimens of 2% Cr and 4% Cr alloy were observed by SEM. Figure 6 illustrates the microstructure apart from fracture surface 2 cm of the ruptured specimens.

The microstructures obtained after stress rupture tests reveal the evidence of coarsening of precipitates in a direction transverse to the applied stress. The comparison of the microstructures shown in Fig. 6 clearly indicates that the average raft thickness varied with Cr content. The adjacent  $\gamma'$  particles met and fused together, thus producing rafts in the 4% Cr alloy. However, it was forming islands and was thus entirely surrounded by the  $\gamma'$  phase in the 2% Cr alloy. The  $\gamma'$  raft of 4% Cr alloy is more regular and perfect than that of 2% Cr alloy. The thickness observed in microstructures decreases with increasing Cr content. This indicates that the coarsening extent of  $\gamma'$  phase of 2% Cr alloy is severer than that of 4% Cr alloy.

The specimens all exhibit the presence of TCP phases in 2% Cr and 4% Cr alloys. Moreover, it has also been shown that the precipitating volume fraction of TCP phases increased with increasing Cr content, which is the same as the result in LTA. It can be seen that the crack initiates and propagates on the TCP phases. High stress concentration at the TCP phase–matrix interfaces or at the points where the TCP precipitates are interlinked is thought to result in the microcracking [16]. It can be concluded that the degeneration of stress rupture



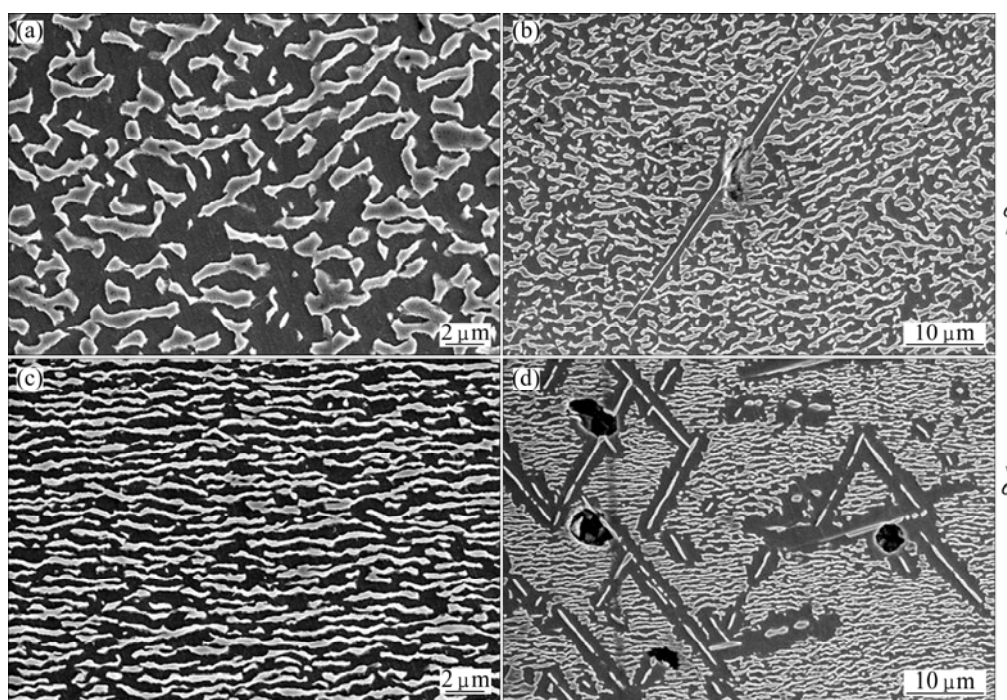


**Fig. 6** Microstructures apart from fracture surface of 2 cm of ruptured specimens: (a), (b) 2% Cr alloy; (c), (d) 4% Cr alloy

properties with increasing Cr content is dominated by the formation of much more TCP phases.

## 4 Conclusions

1) The size of  $\gamma'$  phase particles becomes small and uniform, and the cubic shape turns a little regular with increasing Cr content.

2) The  $\gamma'$  directional coarsening and rafting were observed in the 2% Cr and 4% Cr alloys after LTA at 1100 °C. The rafting rate of  $\gamma'$  phase increased with increasing Cr content. Needle-shaped TCP phases precipitated and grew along fixed direction in both alloys. The precipitating rate and volume fraction of TCP phases significantly increased with increasing Cr content.

3) The tensile property of the alloy increased and the stress rupture properties of the alloy decreased with increasing Cr content at high temperature.

4) The partition ratio of TCP forming elements, Re, W, and Mo increased with increasing Cr content, and the saturation degrees of these elements in  $\gamma$  phases increased. This indicates that the high temperature phase stability of the alloy decreases with increasing Cr content.

## References

- [1] WALSTON W S, O'HARA K, ROSS E W, POLLOCK T M, MURPHY W H. RenéN6: Third generation single crystal superalloy [C]/KISSINGER R D, DEYE D J, ANTON D L, CETEL A D, NATHAL M V, POLLOCK, T M, WOODFORD D A. Superalloys 1996. Warrendale: TMS, 1996: 27–34.
- [2] ERICKSON G L. The development and application of CMSX-10 [C]/KISSINGER R D, DEYE D J, ANTON D L, CETEL A D, NATHAL M V, POLLOCK, T M, WOODFORD D A. Superalloys 1996. Warrendale: TMS, 1996: 35–44.
- [3] ACHARYA M V, FUCHS G E. The effect of long term thermal exposures on the microstructure and properties of CMSX-10 single crystal superalloys [J]. Materials Science and Engineering A, 2004, 381: 143–153.
- [4] CHATTERJEE D, HAZARI N, DAS N, MITRA R. Microstructure and creep behavior of DMS4-type nickel based superalloy single crystals with orientations near [001] and [011] [J]. Materials Science and Engineering A, 2010, 528: 604–613.
- [5] CARON P, KHAN T. Evolution of Ni-based superalloys for single crystal gas turbine blade applications [J]. Aerospace Science Technology, 1999, 3: 513–523.
- [6] ARGENCE D, VERNAULT C, DESVALLEES Y, FOURNIER D. MC-NG: Generation single crystal superalloy for future aeronautical turbine blades and vanes [C]/Superalloys 2000. Warrendale: TMS, 2000: 829–837.
- [7] WALSTON S, CETEL A, MACKAY R, O'HARA K, DUHL D, DRESHFIELD R. Joint development of a fourth generation single crystal superalloy [C]/GREEN K A, POLLOCK T M, HARADA H, HOWSON T W, REED R C, SCHIRRA J J, WALSTON S. Superalloys 2004. Pennsylvania: TMS, 2004: 15–24.
- [8] SATO A, HARADA H, YOKOKAWA T, MURAKUMO T, KOIZUMI Y, KOBAYASHI T, IMAI H. The effect of ruthenium on the phase stability of fourth generation Ni-base single crystal superalloys [J]. Scripta Materialia, 2006, 54: 1679–1684.
- [9] FENG Q, TRYON B, CARROLL L J, POLLOCK T M. Cyclic oxidation of Ru-containing single crystal superalloys at 1100 °C [J]. Materials Science and Engineering A, 2007, 458: 184–194.
- [10] TAN X P, LIU J L, JIN T, SUN X F, HU Z Q. Influence of Cr addition on microstructure of a 5%Re-containing single crystal nickel-based superalloy [J]. Transactions of Nonferrous Metals Society of China, 2011, 21: 1004–1008.

- [11] CHEN J Y, FENG Q, CAO L M, SUN Z Q. Improvement of stress rupture property by Cr addition in Ni-based single crystal superalloys [J]. Materials Science and Engineering A, 2011, 528: 3791–3798.
- [12] CHEN J Y, ZHAO B, FENG Q, CAO L M, SUN Z Q. Effect of Ru and Cr on  $\gamma/\gamma'$  microstructure evolution of Ni-based single crystal superalloys during heat treatment [J]. Acta Metallurgica Sinica, 2010, 46: 897–906. (in Chinese)
- [13] PYCZAK F, NEUMEIER S, GÖKEN M. Influence of lattice misfit on the internal stress and strain states before and after creep investigated in nickel-base superalloys containing rhenium and ruthenium [J]. Materials Science and Engineering A, 2009, 510–511: 295–300.
- [14] CARROLL L J, FENG Q, MANSFIELD J F, POLLOCK T M. Elemental partitioning in Ru-containing nickel-base single crystal superalloys [J]. Materials Science and Engineering A, 2009, 457: 292–299.
- [15] ZHANG J X, MURAKUMO T, KOIZUMI Y, KOBAYASHI T, HARADA H, MASAKI S. Interfacial dislocation networks strengthening a fourth-generation single-crystal TMS-138 superalloy [J]. Metallurgical and Materials Transactions A, 2002, 33: 3741–3746.
- [16] YEH A C, TIN S. Effect of Ru on the high temperature phase stability of Ni-base single crystal superalloys [J]. Metallurgical and Materials Transactions A, 2006, 37: 2621–2631.

## Cr 含量对单晶高温合金显微组织和力学性能的影响

史振学, 刘世忠, 王效光, 李嘉荣

北京航空材料研究院 先进高温结构材料重点实验室, 北京 100095

**摘 要:** 在真空定向凝固炉中制备 Cr 含量分别为 2%和 4%(质量分数)的两种单晶高温合金, 保持其他合金元素含量不变, 研究 Cr 含量对单晶高温合金组织、相稳定性、1100 °C 拉伸性能和 1070 °C、160 MPa 条件下持久性能的影响。结果表明, 随着 Cr 含量的增加, 合金中  $\gamma'$  相尺寸减小, 其均匀化和立方化程度稍有增加。经 1100 °C 长期时效处理后, 两种合金的  $\gamma'$  相都发生了粗化和筏排化, 且筏排化速率随着 Cr 含量的增加而增加。两种合金中都有针状 TCP 相析出, 并沿固定的方向生长, 且 TCP 相的析出速率和析出量随着 Cr 含量的增加而增加。随着 Cr 含量的增加, 合金的高温拉伸性能提高, 而持久性能降低。Cr 含量的增加提高了 TCP 相形成元素 Re、W 和 Mo 在  $\gamma$  基体中的过饱和程度, 因而 Cr 含量的增加降低了合金的高温组织稳定性。

**关键词:** 单晶高温合金; Cr 含量; 显微组织; 相稳定性; 力学性能

(Edited by Wei-ping CHEN)